

# Structural and dielectric properties of the Ruddlesden-Popper $\text{Ba}_2\text{ZrO}_4$ structure from first-principles

Lydie Louis and Serge M. Nakhmanson

Department of Materials Science & Engineering, and Institute of Materials Science,  
University of Connecticut, Storrs, Connecticut 06269, USA\*

Layered variations of the  $\text{ABO}_3$  perovskite structures have gained widespread interest of technological and fundamental importance in view of their inherent properties and functionalities [1–4]. Well-known homologous series of layered oxides based on slabs with (001) perovskite surfaces include Ruddlesden-Popper (RP; structural formula  $\text{A}_{n+1}\text{B}_n\text{O}_{3n+1}$ ), Aurivillius and Dion-Jacobson compounds [3, 4]. Numerous fundamental investigations of their structural, electronic and dielectric properties have led to insights on how to design and tune functional behavior of these materials through strain and interface engineering. Utilizing first-principles-based computational techniques, we have already predicted intriguing behavior in layered-perovskite compounds of the RP type. Specifically, we showed that Goldstone-like states (collective, close to zero frequency excitations, requiring practically no consumption of energy) can be induced in a  $\text{PbSr}_2\text{Ti}_2\text{O}_7$  RP superlattice as easy rotations of the in-plane polarization vector [5]. Furthermore, examination of an (as of now, fictitious) epitaxial  $\text{Ba}_2\text{TiO}_4$  RP compound demonstrated that it exhibits an assortment of competing incommensurate distortions, including ones that promote polarization [6].

Here we focus on exploring the properties of the RP  $\text{Ba}_2\text{ZrO}_4$  structure that displays a yet poorly understood tendency to absorb and desorb small molecules, such as water and  $\text{CO}_2$  [1, 2, 7] (see Figure 1). Therefore, acquiring a greater

insight into the physical underpinnings of the behavior of this compound can result in emergence of useful materials templates for the design of new functional-oxide membranes. This, in turn, will greatly reduce the high energy costs associated with the process of  $\text{CO}_2$  capture and storage [8], thus contributing to the already substantial efforts aimed at developing more advanced technologies for the  $\text{CO}_2$  sequestration.

We have employed a first-principles method based on density-functional theory (DFT) to investigate electronic, vibrational and dielectric properties of the RP  $\text{Ba}_2\text{ZrO}_4$  structure, as well as its phase transformations under applied biaxial strain emulating epitaxial thin-film environment.

The phase space for the system can be separated into four main regions according to the values of  $\varepsilon_s = (a - a_0)/a_0$ , where  $a_0$  is the in-plane lattice parameter of the free standing  $\text{Ba}_2\text{ZrO}_4$  structure with all the normal stress tensor components relaxed to small values: (I) high compressions of above 0.8–1.0%, dominated by incommensurate (IC) distortions; (II) moderate compressions and tensions, where the non-polar  $I4/mmm$  structure is stable; (III) intermediate tensions ranging from 0.5 to  $\sim 3.0\%$ , dominated by combinations of antiferrodistortive (AFD) instabilities; (IV) high tensions of above 3.0–3.5%, with polar distortions being of similar or greater strength than the AFD ones. In comparison, the previously

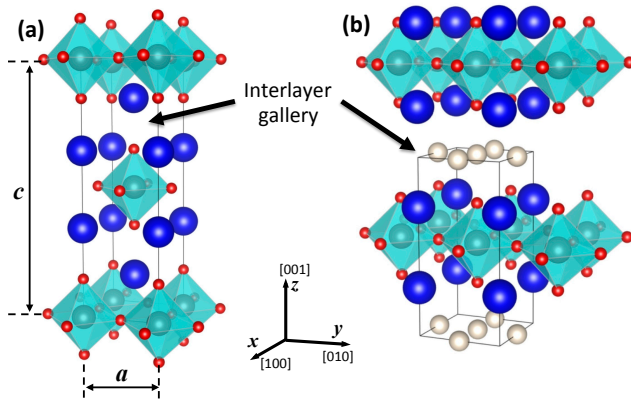


FIG. 1. Molecular intercalation between perovskite-oxide layers. (a) A RP  $\text{A}_2\text{BO}_4$  structure with an empty interlayer gallery (space between the two AO layers) marked by a thick arrow. In-plane and out-of-plane lattice parameters  $a$  and  $c$  of the typical tetragonal unit cell are also shown. (b) Attachment sites for small molecules inside the interlayer gallery of the  $\text{A}_2\text{BO}_4$  structure are indicated by ivory spheres. Notice the difference in layer stackings of the structures depicted in (a) and (b) due to a “layer slide” phase transition.

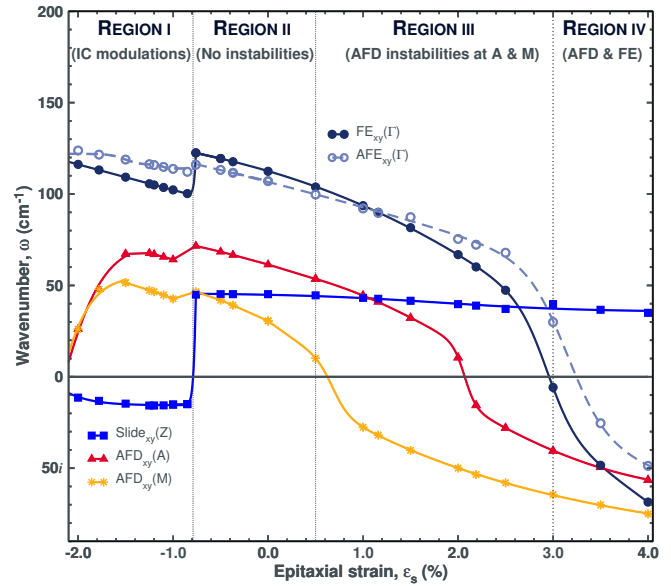


FIG. 2. Soft vibrational modes frequencies  $\omega$  at  $\Gamma$  and various BZ-boundary  $\mathbf{q}$  points as functions of epitaxial strain  $\varepsilon_s$  for  $\text{Ba}_2\text{ZrO}_4$ .

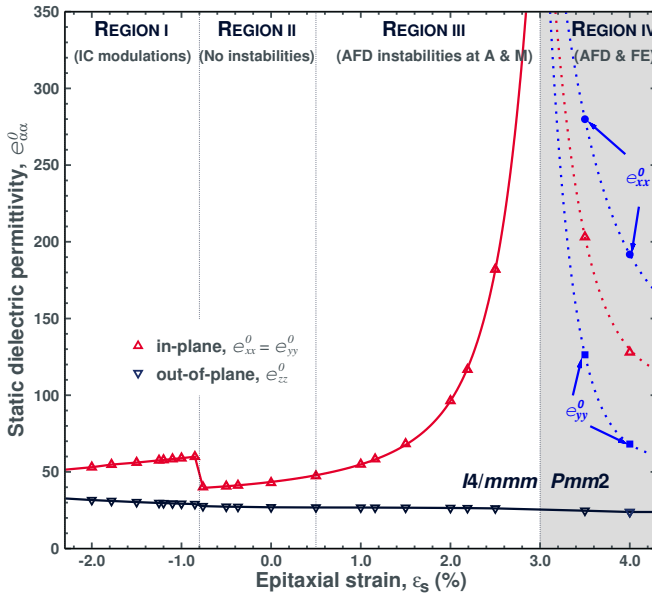


FIG. 3. In- and out-of-plane components of the static dielectric permittivity tensor  $\epsilon_{\alpha\alpha}^0$  computed for the RP  $\text{Ba}_2\text{ZrO}_4$  structure with respect to varying biaxial strain  $\epsilon_s$ . For all compressions and for tensions of less than 3.0% dielectric tensors are computed for the non-polar  $I4/mmm$  configuration, while for larger tensions they are computed for the polar  $Pmm2$  configuration (where  $\epsilon_{xx}^0$  and  $\epsilon_{yy}^0$  are no longer equal by symmetry). Connecting lines are used to guide the eye.

studied case of the RP  $\text{Ba}_2\text{TiO}_4$  [6] is of greater complexity, with IC distortions persisting throughout the whole interval of considered strains and different kinds of IC distortions being possible, as well as their mixing with polar distortions.

In Figure 3 we present the calculated in-plane and out-of-plane components of the static dielectric permittivity tensor  $\epsilon_{\alpha\beta}^0$ . For all the considered compressions and for tensions of less than 3.0% it was done for the non-polar  $I4/mmm$  configuration, while for larger tensions the polar  $Pmm2$  configuration was used. The plot clearly shows the divergence of the in-plane component of the dielectric permittivity tensor at the non-polar to polar phase transition on the boundary between regions III and IV, as well as another minor anomaly upon the lock-in of the IC phase on the boundary between regions I and II. The out-of-plane component of the dielectric permittivity tensor remains approximately the same throughout the region of all the considered epitaxial strains.

Remarkably, though, even after the transition into the polar  $Pmm2$  state the in-plane dielectric permittivity remains unusually high (on the order of 300). We attribute that to the presence of a Goldstone-like excitation [9, 10] in this system, as shown in Figure 4. Although the circular groove in the energy landscape is not as pronounced here as in the case of  $\text{PbSr}_2\text{Ti}_2\text{O}_7$  RP superlattice [5], we can still observe shallow energy minima that are extended in the direction perpendicular to [100] (and other crystallographic directions related by the fourfold rotational symmetry) that allow for easy rotation of

polarization. The nature of this excitation in the RP  $\text{Ba}_2\text{ZrO}_4$  structure — which, unlike the previously studied one, does not contain lead or other lone-pair active ions — is yet unclear and the work to elucidate its origins is currently underway.

\* lydie.louis@uconn.edu

- [1] P. R. Slater and R. K. B. Gover, *J. Mater. Chem.* **11**, 2035 (2001).
- [2] P. R. Slater and R. K. B. Gover, *J. Mater. Chem.* **12**, 291 (2002).
- [3] K. Aleksandrov and V. Beznosikov, *Phys. Solid State* **39**, 695 (1997).
- [4] R. Mitchell, *Perovskites: Modern and Ancient* (Almaz Press, 2002).
- [5] S. M. Nakhmanson and I. Naumov, *Phys. Rev. Lett.* **104**, 097601 (2010).
- [6] W. D. Parker and S. M. Nakhmanson, *Phys. Rev. B* **88**, 035203 (2013).
- [7] R. V. Shpanchenko, E. V. Antipov, and L. M. Kovba, *Zh. Neorg. Khim.* **38**, 599 (1993).
- [8] D. M. D'Alessandro, B. Smit, and J. R. Long, *Angew. Chem. Int. Ed.* **49**, 6058 (2010).
- [9] I. Muševič, R. Blinc, and B. Žekš, *The Physics of Ferroelectric and Antiferroelectric Liquid Crystals* (World Scientific, Singapore, 2000).
- [10] A. D. Bruce and R. A. Cowley, *Structural phase transitions* (Taylor and Francis Ltd., London, 1981).

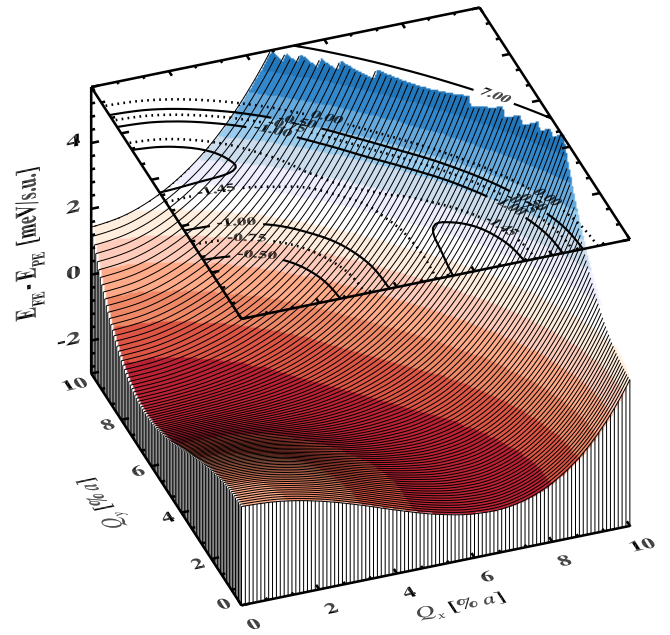


FIG. 4. Energy landscape for the epitaxially strained at  $\epsilon_s = 3.5\%$  RP  $\text{Ba}_2\text{ZrO}_4$  structure with frozen-in doubly degenerate  $\text{FE}_{xy}$  distortions (space group  $Pmm2$ ).  $Q_x$  and  $Q_y$  are the amplitudes of the FE mode eigenvectors polarized along the  $x$ - and  $y$ - axes, respectively. The energy of the paraelectric  $I4/mmm$  phase is taken as zero and  $a$  is the value of the in-plane lattice parameter.